NeuroImage 69 (2013) 126–137

Contents lists available at SciVerse ScienceDirect

NeuroImage

journal homepage: www.elsevier.com/locate/ynimg

Cortical cross-frequency coupling predicts perceptual outcomes

I.C. Fiebelkorn *, A.C. Snyder, M.R. Mercier, J.S. Butler, S. Molholm, J.J. Foxe **

The Sheryl and Daniel R. Tishman Cognitive Neurophysiology Laboratory, Children's Evaluation and Rehabilitation Center (CERC), Departments of Pediatrics and Neuroscience, Albert Einstein College of Medicine, Van Etten Building, 1C, 1225 Morris Park Avenue, Bronx, NY 10461, USA

ARTICLE INFO

Article history:
Accepted 18 November 2012
Available online 24 November 2012

Keywords:
Oscillations
Phase
Cross-frequency coupling
Vision
Sustained attention
EEG

ABSTRACT

Functional networks are comprised of neuronal ensembles bound through synchronization across multiple intrinsic oscillatory frequencies. Various coupled interactions between brain oscillators have been described (e.g., phase-amplitude coupling), but with little evidence that these interactions actually influence perceptual sensitivity. Here, electroencephalographic (EEG) recordings were made during a sustained-attention task to demonstrate that cross-frequency coupling has significant consequences for perceptual outcomes (i.e., whether participants detect a near-threshold visual target). The data reveal that phase-detection relationships at higher frequencies are dependent on the phase of lower frequencies, such that higher frequencies alternate between periods when their phase is either strongly or weakly predictive of visual-target detection. Moreover, the specific higher frequencies and scalp topographies linked to visual-target detection also alternate as a function of lower-frequency phase. Cross-frequency coupling between lower (i.e., delta and theta) and higher frequencies (e.g., low- and high-beta) thus results in dramatic fluctuations of visual-target detection.

Introduction

Identical stimulation does not always lead to the same perceptual and behavioral outcomes. The response to a stimulus depends not only on attributes of the stimulus itself (e.g., its intensity), but also on the "neurophysiological context" at the moment when the stimulus occurs (Arieli et al., 1996; Buzsaki and Chrobak, 1995; Lakatos et al., 2009). This neurophysiological context is defined by the brain's intrinsic spatial and temporal dynamics. That is, normal brain function entails the continual synchronization and desynchronization of neuronal ensembles at various oscillatory frequencies. The perceptual outcome of sensory stimulation depends, in part, on which networks (or brain regions) are engaged when a stimulus occurs, as well as on the excitability state of the neurons embedded in those networks (Boly et al., 2007; Busch and VanRullen, 2010; Busch et al., 2009; Haig and Gordon, 1998; Jansen and Brandt, 1991; Kastner et al., 1999; Lange et al., 2011; Mathewson et al., 2009; Monto et al., 2008; O'Connell et al., 2009; Romei et al., 2008; Sadaghiani et al., 2010; Scheeringa et al., 2011; Varela et al., 1981).

Ongoing oscillations in neuronal ensembles reflect fluctuations in local field potentials between high- and low-excitability states, which can be imagined as the peaks and troughs (or phases) of a sine wave. Several studies have now established that the prestimulus phase of cortical oscillations influences perceptual outcomes (Busch et al., 2009; Dugue et al., 2011; Mathewson et al., 2009). During a high-excitability state, when neurons in the sensory cortices are closer to their firing threshold, a near-threshold stimulus is more likely to be detected and selected for further processing (Lakatos et al., 2007, 2009). Moreover, endogenous (or top-down) signals can modulate the phase of cortical oscillations in anticipation of an expected sensory event (Fiebelkorn et al., 2011; Gomez-Ramirez et al., 2011; Lakatos et al., 2007, 2008). For example, phase can be reset in response to an attended temporal cue, such that a subsequent to-be-detected stimulus optimally aligns with a high-excitability state (and is thus more likely to be detected).

Although it is well-established that the prestimulus phase of ongoing oscillations contributes to perceptual outcomes (i.e., whether a near-threshold stimulus is detected), debate remains over the contribution of oscillations at various frequencies. Some recent studies have demonstrated phase-detection relationships at theta and alpha (4–14 Hz) frequencies (Busch et al., 2009; Dugue et al., 2011; Lakatos et al., 2009; Mathewson et al., 2009). Other studies, which focused on the interaction between attention and visual-target detection, have instead emphasized the importance of low-delta (1–2 Hz) frequencies (Besle et al., 2011; Fiebelkorn et al., 2011; Gomez-Ramirez et al., 2011; Lakatos et al., 2008). Here, we hypothesized that the response to a near-threshold visual-target is influenced by an interaction of ongoing oscillations on multiple temporal scales (i.e., cross-frequency coupling between and within the hubs of functional networks). We therefore sought to

* Correspondence to: I.C. Fiebelkorn, Albert Einstein College of Medicine, Van Etten Building, 1C, 1225 Morris Park Avenue, Bronx, NY 10461, USA. Fax: +1 718 862 1807.
** Correspondence to: J.J. Foxe, Children's Evaluation and Rehabilitation Center (CERC), The Einstein Autism Center of Excellence (Einstein-ACE), Rose F. Kennedy Intellectual & Developmental Disabilities Research Center (IDDRC), Albert Einstein College of Medicine, Van Etten Building, 1C, 1225 Morris Park Avenue, Bronx, NY 10461, USA. Fax: +1 718 862 1807.
E-mail addresses: ianfiebelkorn@gmail.com (I.C. Fiebelkorn), john.foxe@einstein.yu.edu (J.J. Foxe).

1053-8119/$ – see front matter © 2012 Elsevier Inc. All rights reserved.
http://dx.doi.org/10.1016/j.neuroimage.2012.11.021

(1) establish which frequencies are most closely tied to visual-target detection and (2) define the temporal and spatial relationships among those frequencies.

Materials and methods

Participants

Seven neurologically normal volunteers participated in the experiment (mean age 30.3 ± 3.6 years; 1 female; 1 left-handed), and data from all participants were included in the analyses. The Institutional Review Board of the Albert Einstein College of Medicine approved the experimental procedures. Written informed consent was obtained from all participants prior to data collection, in line with the Declaration of Helsinki.

Stimuli and task

The experiment was administered in a light- and sound-attenuated chamber using Presentation software version 14.4 (Neurobehavioral Systems, Albany, CA, USA). All stimuli were presented on a 34.5 × 55.0 cm LCD monitor with a 60-Hz refresh rate (ViewSonic, model VP2655wb). Fig. 1 provides a schematic of the experimental task. Participants, who were positioned 70 cm in front of the monitor, were asked to maintain central fixation and report the occurrence of a near-threshold visual target: a sine wave grating (3 cycles per degree) with 16-ms duration, subtending 2.5° of the visual angle in both the vertical and horizontal planes. The visual target was presented 2° below central fixation, and a sound (1000 Hz) with 16-ms duration was presented from a BOSE (Companion 2) speaker positioned directly below the monitor.

After the participant clicked the right mouse button to begin a trial, there was a 3–5 second prestimulus interval, which was followed by a clearly audible sound (~65 dB SPL). The visual stimulus might co-occur with the sound (35%) or it might occur anytime up to 5 s thereafter (45%). Catch trials (20%), where there was a sound presented at the beginning of the trial but no visual target was presented throughout the duration of the trial, were included to estimate false alarms. Participants were directed to click the left mouse button whenever they detected a visual stimulus, regardless of when it occurred. Trials ended either when the participant responded or 6 s after the sound was presented (giving participants enough time to respond to a visual stimulus that occurred at 5 s after the sound). An SR Research EyeLink eye tracker was used to discard all trials with blinks or eye movements.

To maintain vigilance, each participant's time in the experiment was distributed over 2 days. On each day, participants completed 4 blocks, with each block consisting of 120 self-paced trials. After every 20 trials, participants were updated on their behavioral performance. At the end of these mini-blocks, the contrast of the visual target was adjusted to guarantee that overall behavioral performance would be pinned at approximately 50%. That is, if a participant's hit rate in the preceding mini-block exceeded 60%, the contrast of the visual target was decreased; if a participant's hit rate fell below 40%, or if a participant committed more than two false alarms, the contrast of the visual target was increased. The average hit rates reported in the present manuscript are only based on trials that occurred at least 2.5 s after the auditory cue and therefore might be higher or lower than 50% (Fig. 3).

Electroencephalogram (EEG) recording

Continuous EEG was acquired through the ActiveTwo BioSemi (Amsterdam, the Netherlands) electrode system from 160 scalp electrodes, digitized at 512 Hz with a 31.25 nV quantization resolution. Data were band-passed filtered during acquisition from 0.1 to 100 Hz. With the BioSemi system, every electrode or combination of electrodes can be assigned as the reference, which is done purely in software after acquisition. BioSemi replaces the ground electrodes that are used in conventional systems with two separate electrodes: Common Mode Sense active electrode and Driven Right Leg passive electrode. These two electrodes form a feedback loop, which drives the average potential of the participant as close as possible to the reference voltage of the analog-to-digital converter, thus rendering them references.

Data processing

EEG data were processed using the FieldTrip toolbox (Donders Institute for Brain, Cognition, and Behaviour, Radboud University Nijmegen, the Netherlands) for MATLAB (The MathWorks, Natick, MA, USA). Here, our goal was to investigate the link between prestimulus phase (at multiple frequencies) and visual-target detection during a sustained-attention task. We therefore needed to obtain an accurate measure of phase on each trial for all frequencies of interest: 1–25, 30, 35, 40, 45, and 50 Hz. Before measuring prestimulus phase, however, we first divided the continuous EEG into epochs, from −3 s prior to the auditory cue to 0.5 s after the visual target was presented. These epochs were detrended, and baseline corrected based on the mean voltage over the entire trial. The EEG data were then filtered using a discrete Fourier transform (DFT) filter to remove 60-Hz line noise. In addition to removing trials with blinks or eye movements based on eye tracking data, an artifact rejection criterion of ± 100 μV was employed at all the electrodes to reject trials with excessive EMG, or other noise transients. Following artifact rejection, the epochs were re-referenced to an average reference (i.e., an average of the activity at all electrodes).

To measure prestimulus phase, we used frequency-specific Morlet wavelets that varied in the number of cycles, from 2 cycles at 1Hz, 3 cycles at 2 Hz, 4 cycles at 3 Hz, 5 cycles at 4 Hz, 6 cycles at 5 Hz, and 7 cycles for all of the other frequencies. We varied the number of cycles to avoid contamination from the auditory evoked potential that occurred in response to the auditory cue. Each wavelet has a temporal extent based on the frequency and number of cycles. For example, a 1-Hz wavelet with 2 cycles extends for 2 s. To limit the

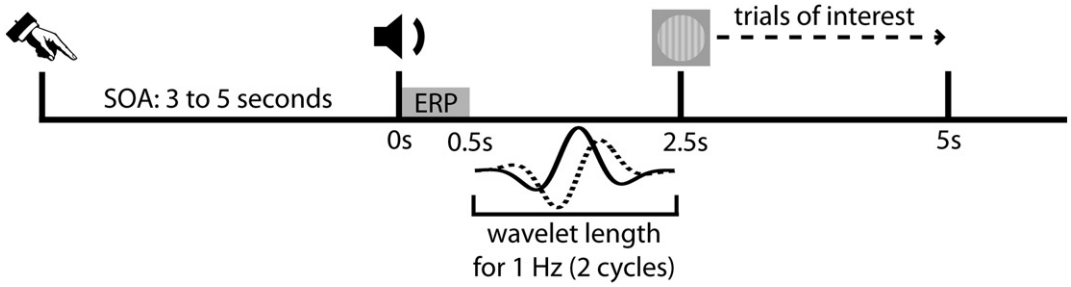

Fig. 1. A schematic of the sustained attention task. Participants reported the occurrence of near-threshold visual targets. The present analysis is restricted to trials when the visual target occurred at least 2.5 s after the auditory cue.

overlap between our phase measurements and the evoked potential that occurred in response to the auditory cue, we only examined the link between prestimulus phase and visual-target detection during trials where the visual target occurred at least 2.5 s after the sound (Fig. 1). After excluding trials where the visual target either co-occurred with the sound or occurred less than 2.5 s after the sound, an average of 196 trials per participant remained. For these trials, the wavelet for each frequency was fit such that the last time point included in the phase measurement was the time point just prior to visual-target presentation. Wavelets never overlapped with the response to visual targets, and never included time points within 0.5 s of the sound. Prestimulus phase measurements were calculated based on the complex output of the wavelet convolution.

Measuring phase-detection relationships

Fig. 2 illustrates the procedure we used to measure the change in visual-target detection as a function of phase at all electrodes and frequencies of interest, both independent of other frequencies (Step 1) and taking into account cross-frequency coupling between lower and higher frequencies (Step 2). We first calculated the hit rate for all trials where the prestimulus phase fell within one-half of the

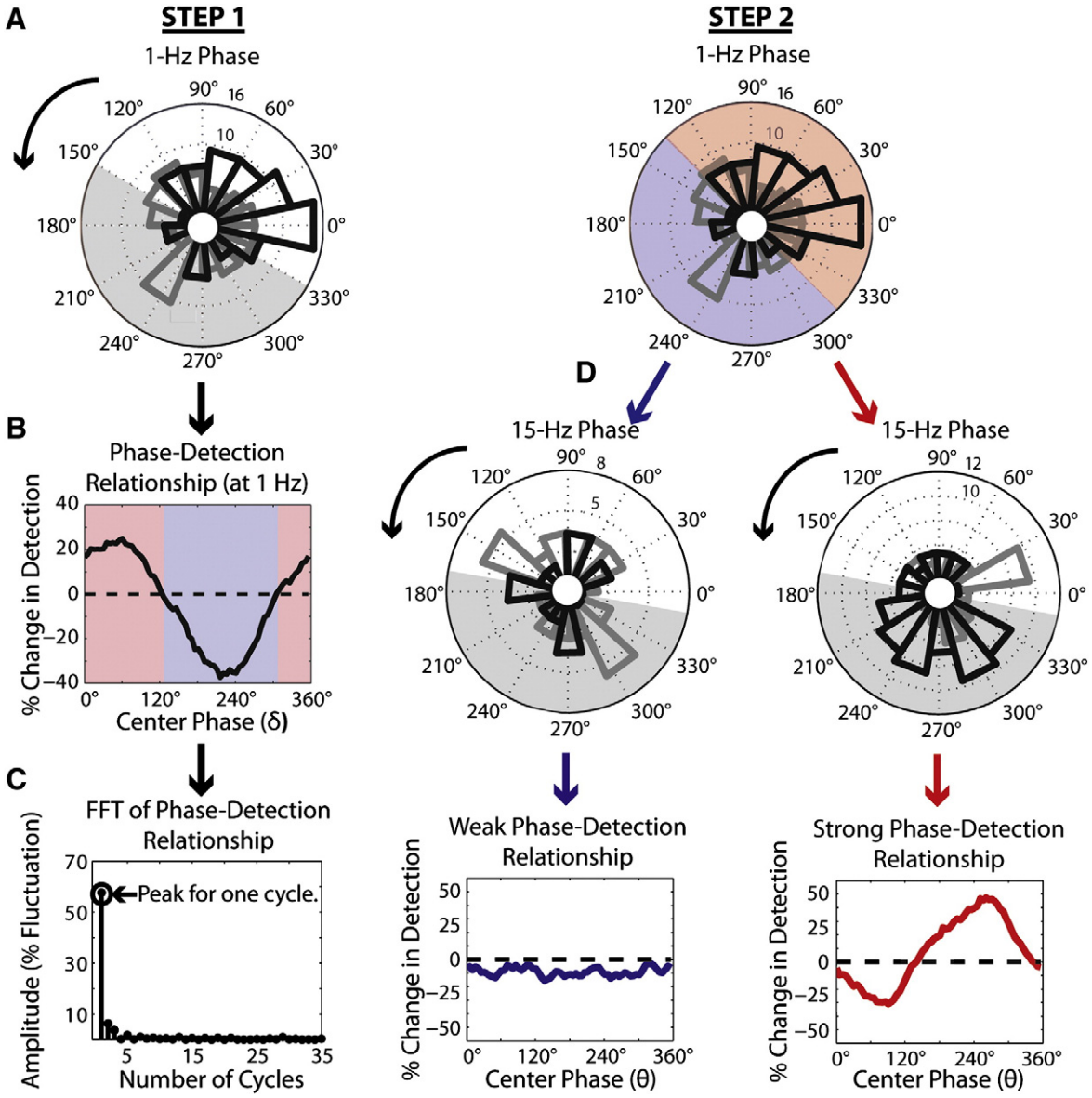

Fig. 2. A schematic of the procedures for establishing phase-detection relationships, both independent of other frequencies (Step 1) and taking into account cross-frequency coupling between lower and higher frequencies (Step 2). (A) The hit rate was calculated across trials where the prestimulus phase fell within one-half of the unit circle. This procedure was repeated, with the 180° arc being rotated around the unit circle in 5° steps. (B) The resulting 72 phase-specific hit rates were then converted to a percent change in visual-target detection relative to the overall hit rate, revealing a phase-detection relationship. (C) To describe this phase-detection relationship with a single number, the data were transformed into the frequency domain. The FFT peak associated with one cycle (i.e., the peak that describes a biphasic relationship) represents the fluctuation in hit rates as a function of prestimulus phase, and thus our dependent measure. (D) To determine whether the phase of lower frequencies modulates phase-detection relationships at higher frequencies, we used the same analysis steps (A–C) after first binning trials based on the prestimulus phase of either delta or theta oscillations. Trials were split into two bins: (1) a "good" bin, centered on the phase of the lower-frequency with the highest likelihood of visual-target detection (represented with red), and (2) a "bad" bin, centered on the phase of the lower-frequency with the lowest likelihood of visual-target detection (represented with blue). The data displayed here were taken from Participant 3.

unit circle (Fig. 2A). This 180° arc of prestimulus phases was then rotated around the unit circle, with the hit rate being calculated in 5° steps (i.e., we calculated 72 phase-specific hit rates for each electrode and frequency of interest). Based on volume conduction of the EEG signal, we posited that any relationship between prestimulus phase and visual-target detection would have some physiologically plausible spatial extent (i.e., such a relationship should not be limited to a single electrode). For each frequency of interest, we therefore conservatively averaged the phase-specific hit rates at each electrode with the phase-specific hit rates from its 4 closest neighbors. No such smoothing was applied to our statistical simulations (see below). Because it was not possible to fully sample the surrounding area of the scalp, we eliminated the 24 electrodes positioned around the edge of the cap from the remainder of the analysis. We next normalized the spatially smoothed phase-specific hit rates relative to the participant-specific overall hit rate. That is, the data were transformed from hit rates into a percent change in visual-target detection. The results of this analysis could then be plotted to illustrate visual-target detection as a function of prestimulus phase (Fig. 2B).

To obtain a single measure of the strength of the phase-detection relationship at each electrode and frequency of interest, we next conducted a spectral analysis of the 72-point series that resulted from the preceding step (i.e., visual-target detection as a function of phase) using the fast Fourier transform (FFT). Assuming that the phase-detection relationship would be biphasic (i.e., with an optimal phase where the likelihood of visual-target detection would be at a maximum and a suboptimal phase where the likelihood of visual-target detection would be at a minimum), we kept the amplitude measurements associated with one cycle (Fig. 2C). This output is equivalent to the percent fluctuation in visual-target detection attributable to prestimulus phase, and therefore captured the strength of the phase-detection relationship with a single value. Using the FFT instead of simply subtracting the maximum increase in performance from the minimum decrease in performance had two important consequences: (1) it guaranteed that the peaks and troughs of the phase-detection relationships would be separated by approximately 180° (i.e., it constrained the phase-detection relationship to be sinusoidal), and (2) it eliminated any high-frequency noise that would artificially inflate the magnitude of the hypothesized phase-detection relationship.

After determining the strength of the phase-detection relationship at each electrode and frequency of interest, we next investigated whether phase-detection relationships at higher frequencies were dependent on the phases of either delta or theta oscillations (i.e., we measured cross-frequency coupling). To do this, we used the following procedure: (1) we binned trials based on the prestimulus phase of either delta or theta oscillations (Fig. 2D), and (2) for each of the higher frequencies outside those frequency bands (i.e., 5–30 Hz and 10–30 Hz, respectively), we calculated phase-detection relationships (Figs. 2A–C) separately for each of the two delta- or theta-phase bins. The specific delta and theta frequencies that we used to bin trials, 1 Hz and 9 Hz, were chosen based on peaks in the population-level results from Step 1 (Fig. 3). Here, we refer to 9 Hz as theta, but it could also be classified as low alpha. The prestimulus phase measurements that were used to bin trials based on lower-frequency phase were taken from the participant-specific electrode with the strongest phase-detection relationship (at the lower frequency). Exactly the same procedure was followed during our non-parametric statistical approach. Each bin included trials where prestimulus phase measurements fell within one-half of the unit circle (Fig. 2D). The center phases of these delta- and theta-phase bins were the phases with the highest ("good" bin) and lowest ("bad" bin) likelihood of visual-target detection (from Step 1, Fig. 2B). As a final step, we measured the absolute value of the difference in the phase-detection relationships between the two delta- or theta-phase bins. That is, we measured whether the phase of lower frequencies modulated phase-detection relationships at higher frequencies.

To test the hypothesis that phase-amplitude coupling might account for the observed link between the phase of lower frequencies and phase-detection relationships at higher frequencies, we also tested whether amplitude measurements for the higher frequencies varied between the delta- or theta-phase bins. This analysis was limited to the maximal electrodes where phase-detection relationships at higher frequencies were most strongly modulated by the phase of delta or theta oscillations.

Statistical analysis

We used non-parametric procedures at the single-participant and population levels to quantify statistical confidence. Non-parametric statistics are robust to violations of assumptions for parametric statistical tests, such as normally-distributed sampling distributions and homogeneity of variance. The p-value for a non-parametric test is the proportion of values in the reference distribution that exceed the test statistic (i.e., the observed value from our collected data). For all statistical comparisons in the present study, we adopted an alpha criterion of 0.05. That is, after corrections for multiple comparisons (see below), corrected p-values were considered to be significant if they were less than 0.05.

We first tested whether visual-target detection varied significantly as a function of prestimulus phase (i.e., whether there were significant phase-detection relationships). For each electrode and all frequencies of interest, we generated reference distributions by randomizing the phase measurements across trials, and then following our general procedure for determining the strength of the phase-detection relationship (see above). In other words, we ran the exact same data through the identical analysis steps with the pairings of phase to behavior randomized. After 1000 iterations, we had a distribution of randomized measures to compare with the observed phase-detection relationships.

We next tested whether phase-detection relationships at higher frequencies were dependent on the phases of delta or theta. Here, we wanted to establish whether binning trials based on the phase of either delta or theta would generate significant differences in the strength of the phase-detection relationships at higher frequencies (i.e., whether the strength of the phase-detection relationship would differ between the two bins). To generate reference distributions, we randomized the phase measurements for either delta or theta, and then followed the standard analysis procedure (Fig. 2). Phase measurements for the higher frequencies were not randomized. Again, all of the reference distributions were based on 1000 iterations.

Finally, we tested whether amplitude measurements at the higher frequencies differed significantly between the delta- or theta-phase bins. We again randomized the phase measurements for either delta or theta, and followed the standard binning procedure, with the dependent measure now being amplitude at the higher frequency rather than phase-detection relationships at the higher frequency.

To test statistical significance at the population level (for each analysis step), we randomly sampled values from each participant's surrogate data distribution, averaged these values, and thus created a population-level surrogate data distribution. To further control for potential outliers in our observed data (i.e., to account for variability across participants), we converted the observed and randomized population-level averages into z-scores (Groppe et al., 2011).

Multiple comparisons

Here we measured phase-detection relationships across multiple frequencies and electrodes. To control for false positives, all p-values were corrected using the false discovery rate procedure developed by Benjamini and Hochberg (1995), which has been frequently employed by neuroimaging studies (Genovese et al., 2002). This correction, a sequential Bonferroni-type procedure, is highly conservative and thus favors certainty (Type II errors) over statistical power (Type I errors).

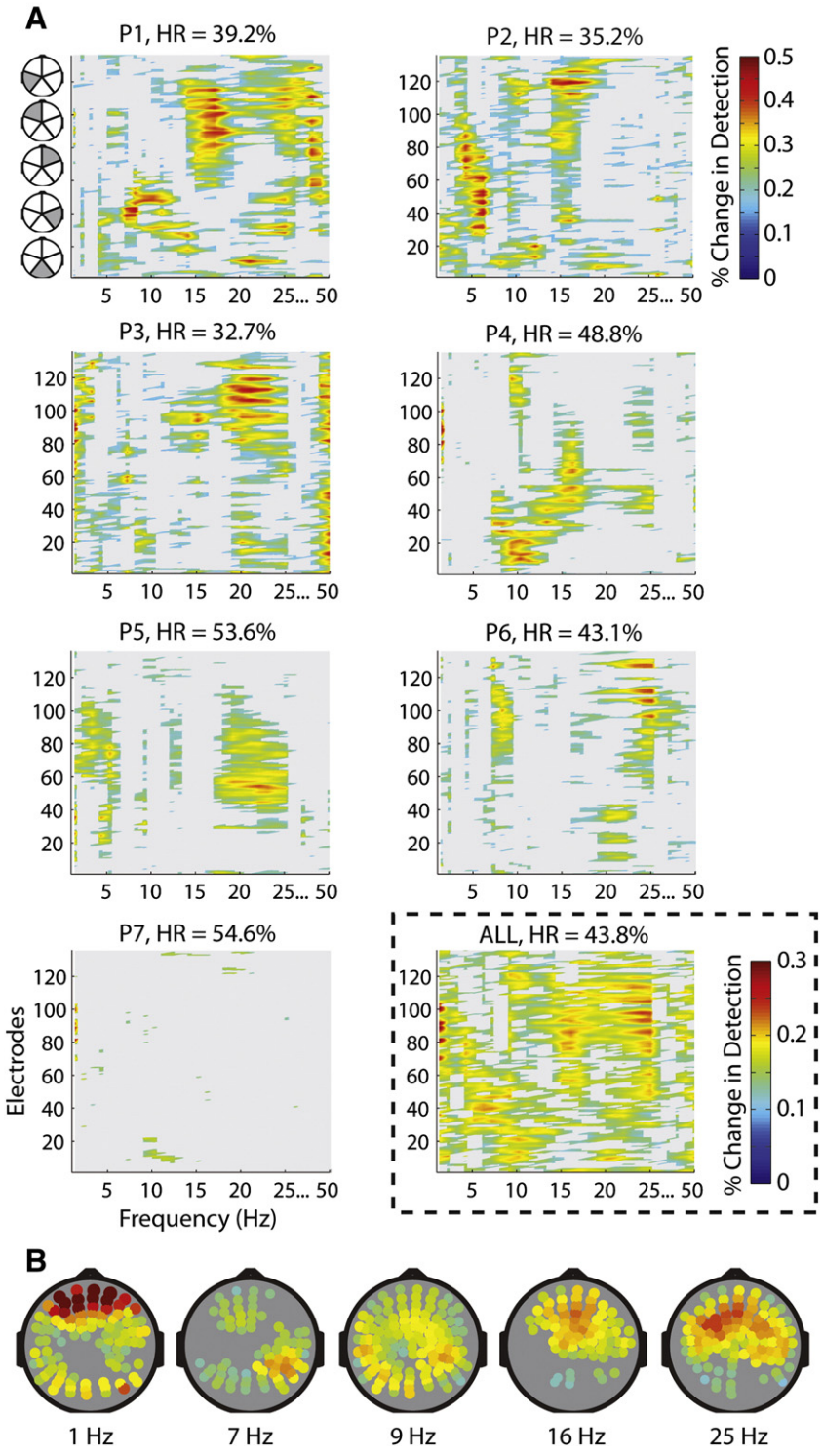

Fig. 3. There is a strong link between prestimulus phase and visual-target detection at multiple frequencies. (A) Significant phase-detection relationships across electrodes and frequencies at the participant and population levels. A gray mask covers insignificant (corrected p-value ≥0.05) phase-detection relationships. Average hit rates (HR) are provided to better interpret phase-dependent swings in visual-target detection. (B) Corresponding scalp topographies are shown for the peak frequencies at the population level. Only electrodes with significant (corrected p-value <0.05) phase-detection relationships are plotted. The size and color of the electrodes represent the strength of the phase-detection relationship.

We employed corrections for multiple comparisons across frequencies and electrodes at all levels of analysis, for both participant- and population-level statistics. After corrections for multiple comparisons, the alpha criterion was set at 0.05. The reported results were further constrained by assuming a biphasic relationship between phase and visual-target detection. That is, we only considered phase-dependent modulations of visual-target detection where the peak in performance was 180 degrees from the trough.

Results

Here, we investigated the influence of prestimulus oscillatory phase on visual-target detection during a sustained attention task (Fig. 1). To ensure accurate phase measurements, our analysis was limited to trials when the near-threshold visual target occurred at least 2.5 s after the auditory cue (thus avoiding contamination from the auditory evoked potential). For each trial of interest, we used 30 frequency-specific wavelets (1–25, 30, 35, 40, 45, and 50 Hz) to estimate the phase of ongoing oscillations just prior to visual-target presentation. We then combined these prestimulus phase measurements with behavioral data to establish whether phase at various frequencies influenced the likelihood of visual-target detection (Fig. 2). For this purpose, we examined fluctuations in hit rates as a function of the prestimulus phase at each electrode. This procedure revealed both optimal and suboptimal phases for visual-target detection.

Fig. 3 displays phase-detection relationships at each electrode and frequency of interest. For all seven participants, the peak in the phase-detection relationship within the delta band occurred at 1 Hz. The fluctuation in visual-target detection as a function of prestimulus phase at 1 Hz ranged from 36–58% (at the participant-specific electrode with the strongest phase-detection relationship). Moreover, the phase-detection relationship at 1 Hz remained strong after averaging across the participants (i.e., at the population level), confirming that low-delta oscillations play an important role in perceptual outcomes. These results are thus in good agreement with Fiebelkorn et al. (2011), who used a psychophysical approach and the same task to suggest that visual-target detection itself oscillates at approximately 1 Hz, at least under conditions of sustained attention.

The fluctuation in visual-target detection as a function of prestimulus phase at participant-specific peaks in the theta band ranged from 31 to 48% (at the participant-specific electrode with the strongest phase-detection relationship). Averaging our results across participants revealed two consistent peaks within the theta (or theta/low alpha) band, at both 7 Hz and 9 Hz. These results thus lend further support to previous studies describing significant phase-detection relationships within the theta (or theta/low alpha) band (Busch and VanRullen, 2010; Busch et al., 2009; Mathewson et al., 2009).

Fig. 3 confirms that the phases of both delta and theta oscillations strongly influence the likelihood of visual-target detection (corrected p-values <0.05). But there were also consistent phase-detection relationships at higher frequencies, with additional peaks in the low- and high-beta bands. In other words, hit rates varied significantly as a function of prestimulus phase across a wide range of oscillatory frequencies. It should be noted that the participant with the weakest evidence of a link between oscillatory phase and visual-target detection outside the low-delta range (i.e., P7) was the participant who required the highest contrast visual target to attain 50% performance (i.e., 50% performance across the entire response period, including trials when the visual target either co-occurred with the auditory cue or occurred within 2.5 s of the auditory cue). We hypothesize that the influence of oscillatory phase on visual-target detection gets stronger with weaker stimulation. That is, the stronger the stimulation, the more likely it is that the response will clear the threshold for detection, regardless of whether perceptually relevant oscillations are at a high- or low-excitability phase.

Previous research has shown that brain rhythms do not operate in isolation, instead interacting on multiple temporal and spatial scales (Canolty and Knight, 2010; Jensen and Colgin, 2007). For example, a number of studies have demonstrated that the phase of theta oscillations modulates the amplitude of gamma (>30 Hz) oscillations (Bragin et al., 1995; Canolty et al., 2006; Csicsvari et al., 2003; Lakatos et al., 2005; Whittingstall and Logothetis, 2009). Here, we next investigated whether the strength of phase-detection relationships at higher frequencies was dependent on the phases of lower frequencies (i.e., delta and theta).

To examine such cross-frequency coupling, we first separated trials into two bins based on the prestimulus phase of either delta (1 Hz) or theta oscillations (9 Hz). For each of the higher frequencies, we then compared phase-detection relationships across these lower-frequency phase bins. Fig. 2 reveals typical results from this procedure (Step 2), displaying phase-detection relationships at 15 Hz in each of two delta-phase bins (for Participant 3). These data were taken from the electrode with the largest difference (at 15 Hz) between the bins. In one delta-phase bin (i.e., the "strong" bin), there was a 70% fluctuation in visual-target detection as a function of prestimulus phase. In the other delta-phase bin (i.e., the "weak" bin), there was absolutely no fluctuation in visual-target detection as a function of prestimulus phase. Fig. 4 summarizes the results of this cross-frequency analysis across electrodes and frequencies, displaying significant (corrected p-values <0.05) delta-dependent phase-detection relationships, at both the single-participant and the population levels. Fig. 5 displays the corresponding significant (corrected p-values <0.05) theta-dependent phase detection relationships, again at both the single-participant and the population levels. These figures depict the difference in the phase-detection relationships between the "good" and "bad" delta- and theta-phase bins (i.e., the bins centered on the phases at which the lower frequency had the highest and lowest likelihood of visual-target detection). Frequencies within the theta and beta bands typically had a strong phase-detection relationship at one phase of the 1-Hz oscillation (i.e., delta), and a much weaker phase-detection relationship at its opposite phase. Similarly, frequencies within the low- and high-beta bands typically had a strong phase-detection relationship at one phase of the 9-Hz oscillation (i.e., theta), and a much weaker phase-detection relationship at the opposite phase. These data therefore demonstrate that phase-detection relationships at higher frequencies can be strongly dependent on the phases of both delta and theta.

One possible explanation for the observed link between the phase of lower frequencies and the strength of phase-detection relationships at higher frequencies is phase-amplitude coupling. In the context of the present experiment, a prediction of phase-amplitude coupling would be that the amplitude of the higher-frequency oscillation is greater during a certain phase of the lower-frequency oscillation, and thus the higher-frequency oscillation has a strong influence on perceptual outcomes during this phase. On the other hand, the amplitude of the higher-frequency oscillation is diminished during the opposite phase of the lower-frequency oscillation, and thus the higher-frequency oscillation has a weak influence on perceptual outcomes during this opposite phase.

To test whether phase-amplitude coupling might be underlying the cross-frequency relationships observed in perceptual outcomes, we compared amplitude measurements across our delta- and theta-phase bins. In other words, we investigated whether higher frequencies had greater amplitude in the bin with a strong phase-detection relationship (relative to the bin with a weak phase-detection relationship). This analysis was focused on the electrodes where phase-detection relationships at higher frequencies were most strongly modulated by the phase of delta and/or theta oscillations. Following delta-phase binning, amplitude measurements differed significantly ($p<0.05$) between bins at the theta peaks for three of the seven participants (Participants 1, 3, and 6). There were no significant differences between bins at any of the delta-binned beta peaks. Following theta-phase binning, amplitude measurements only differed significantly at one participant's high-beta peak (Participant 6). These results suggest that, in the context of the present experimental paradigm, phase-amplitude coupling might play a very limited role in determining the link between the phase of lower frequencies and the strength of phase-detection relationships at higher frequencies.

It should be noted that phase measurements are less reliable as the amplitude of oscillatory activity decreases (i.e., phase measurements become less precise). Phase-detection relationships at high frequencies might therefore seem to be weaker during periods of lower oscillatory

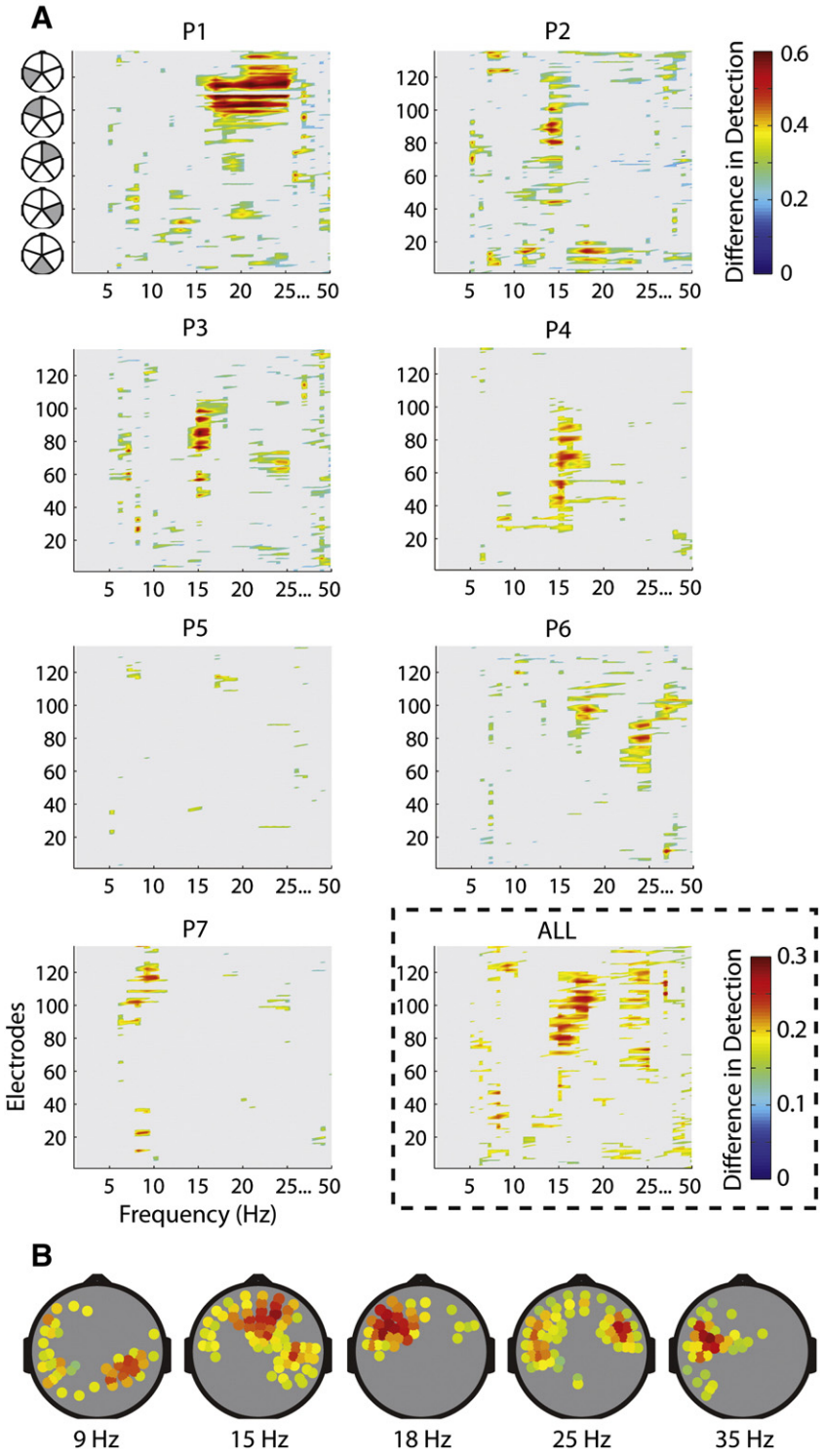

Fig. 4. Cross-frequency coupling between delta (1 Hz) and higher frequencies is strongly linked to perceptual outcomes. (A) Significant differences between delta-phase bins across electrodes and frequencies at the single-participant and population levels. A gray mask covers insignificant (corrected p-value ≥0.05) phase-detection relationships. (B) Corresponding scalp topographies are shown for the peak frequencies at the population level. Only electrodes with significant differences (corrected p-value <0.05) in the phase-detection relationships between the delta-phase bins are plotted. The size and color of the electrodes represent the magnitude of the difference (in the phase-detection relationship) between the delta-phase bins.

amplitude, but these weaker phase-detection relationships might simply result from less reliable phase measurements. Considering the present data, however, a relationship between the amplitude of oscillatory activity and the reliability of phase measurements is unlikely to explain the cross-frequency results for a couple of reasons: (1) as stated in the previous paragraph, we only rarely found that the amplitude of the higher frequency oscillation varied across the lower-frequency phase bins, and (2) on the rare occasion that there was a significant difference

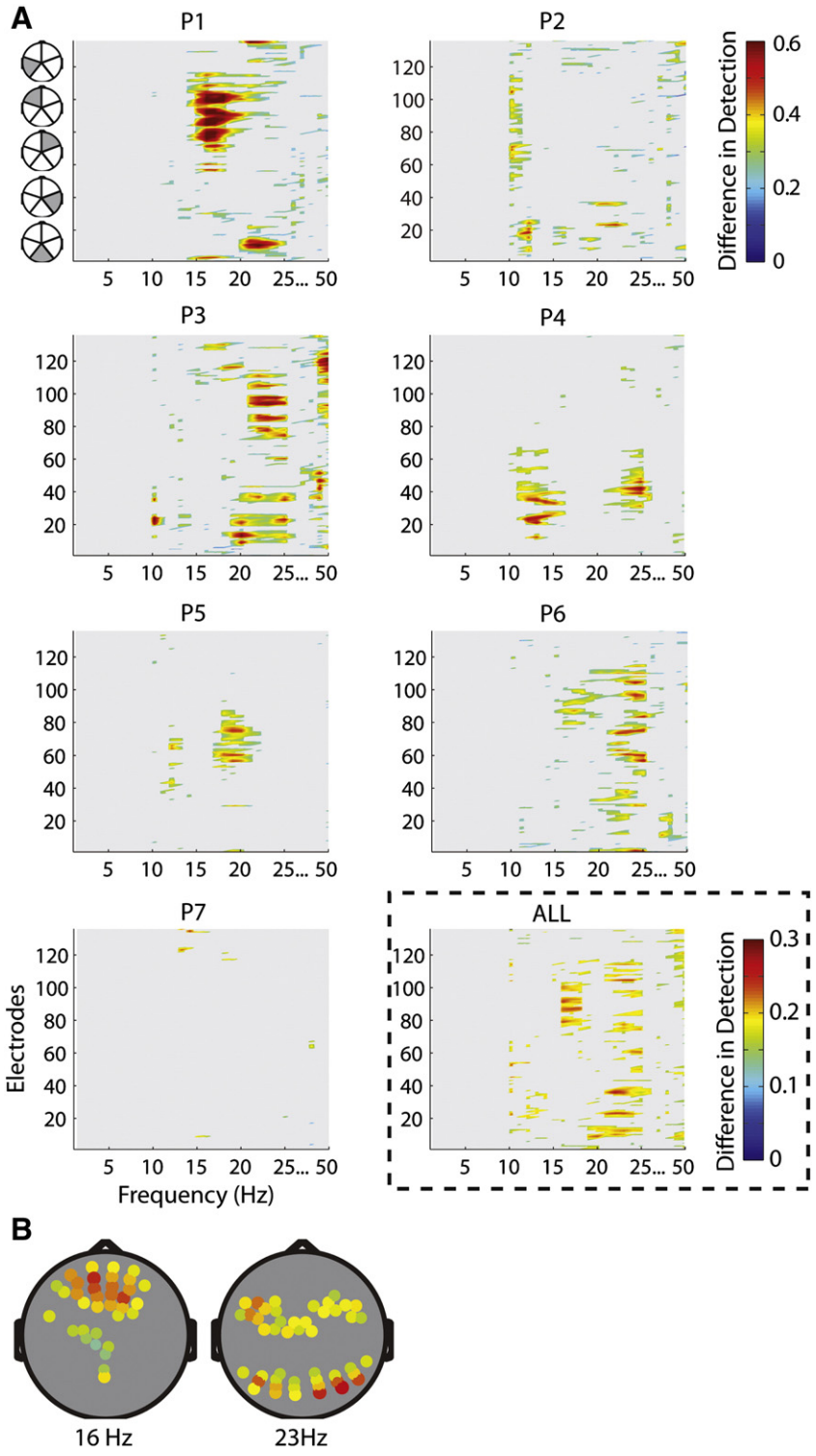

Fig. 5. Cross-frequency coupling between theta (9 Hz) and higher frequencies is strongly linked to perceptual outcomes. (A) Significant differences between theta-phase bins across electrodes and frequencies at the single-participant and population levels. A gray mask covers insignificant (corrected p-value ≥0.05) phase-detection relationships. (B) Corresponding scalp topographies are shown for the peak frequencies at the population level. Only electrodes with significant differences (corrected p-value <0.05) in the phase-detection relationships between the theta-phase bins are plotted. The size and color of the electrodes represent the magnitude of the difference (in the phase-detection relationship) between the theta-phase bins.

in the oscillatory amplitude between the two lower-frequency phase bins, the stronger phase-detection relationship sometimes occurred during the bin with lower oscillatory amplitude.

Oscillations measured at the scalp reflect synchronization of neuronal activity within both local and long-range networks, and the specific networks that are engaged at the moment a stimulus occurs influence perceptual outcomes (Boly et al., 2007; Kastner et al., 1999; McMains et al., 2007; Sadaghiani et al., 2010). A closer look at the present results indicates that the specific higher frequencies and scalp topographies (i.e., the neurophysiologic context) linked to visual-target detection alternate as a function of lower-frequency phase. Whereas Figs. 4 and 5 present the absolute value of the difference between the delta-

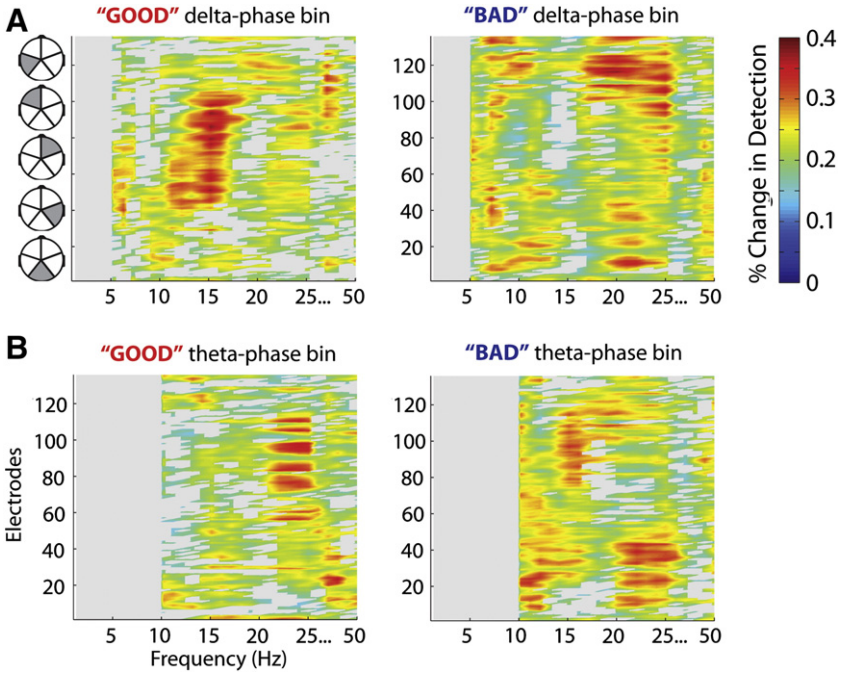

Fig. 6. The specific frequencies and scalp topographies predicting visual-target detection shift as a function of lower-frequency phase. Population-level results depicting significant (A) delta- and (B) theta-dependent phase-detection relationships (at higher frequencies) during both the "good" and "bad" phases of the lower-frequency oscillation. A gray mask covers insignificant (corrected p-value ≥ 0.05) phase-detection relationships. Higher frequencies can be highly predictive of visual-target detection during either the lower frequency's optimal phase (i.e., the phase with the highest likelihood of visual-target detection) or the lower frequency's suboptimal phase (i.e., the phase with the lowest likelihood of visual-target detection).

or theta-phase bins, Fig. 6 instead displays the phase-detection relationships (at the population level) separately for each bin (corrected p-values <0.05). These results indicate that one set of higher frequencies and brain regions determined the likelihood of visual-target detection during the "good" phase of the delta or theta oscillations (i.e., the phase with the highest likelihood of visual-target detection), and a different set of higher frequencies and brain regions determined the likelihood of visual-target detection during the "bad" phase of the delta or theta oscillations (i.e., the phase with the lowest likelihood of visual-target detection).

Whereas the link between the phase of lower frequencies and phase-detection relationships at higher frequencies does not seem to result from phase-amplitude coupling, Fig. 6 suggests an alternative explanation: phase-frequency coupling (Jensen and Colgin, 2007). Phase-detection relationships in a given brain region tended to shift to a higher frequency during the "good" (or optimal) phases of the delta and theta oscillations relative to during the "bad" (or suboptimal) phases of the delta and theta oscillations. For example, the phase of frontal beta oscillations was strongly linked with visual-target detection during both phases of the theta oscillation; however, during the "bad" phase, the peak in the beta band occurred at ~15 Hz, and during the "good" phase, the peak in the beta band occurred at ~25 Hz (Fig. 6B). For delta-dependent phase-detection relationships, a similar pattern of results was apparent over left frontal regions (Fig. 6A). Here, the frequency linked to visual-target detection shifted from ~25 Hz during the "bad" phase of the delta oscillation to ~35 Hz during the "good" phase of the delta oscillation.

Discussion

Research on perception has traditionally focused on the brain's response to external stimulation and how that response varies as a function of stimulus attributes (e.g., intensity). The focus of more recent research has been broadened to also consider the internal state of the brain at the moment a stimulus occurs. This "neurophysiological context" can be described in two ways: (1) spatially (i.e., which functional networks are engaged?) and (2) temporally (i.e., what is the phase of synchronized activity within those functional networks?). These two dimensions of the neurophysiological context are not independent, as different cortical distances have been associated with different oscillatory frequencies. Local synchronization tends to occur at higher frequencies (Fries et al., 2001; Gray et al., 1989) and long-range synchronization tends to occur at lower frequencies (von Stein and Sarnthein, 2000). Here, we investigated how prestimulus phase across a wide range of oscillatory frequencies influences perceptual outcomes.

Our results reveal that visual-target detection varies strongly as a function of prestimulus phase on multiple temporal scales, from low-delta to high-beta frequencies. These data therefore extend previous findings that described a relationship between phase—within delimited frequency bands—and either behavioral or neurophysiological outcomes (Busch et al., 2009; Dugue et al., 2011; Haig and Gordon, 1998; Jansen and Brandt, 1991; Kayser et al., 2008; Kruglikov and Schiff, 2003; Lakatos et al., 2007, 2009; Makeig et al., 2002; Mathewson et al., 2009; Monto et al., 2008; Scheeringa et al., 2011). Many of these studies highlighted the role of theta/low alpha oscillations. We confirm the importance of this frequency band, but also reveal low-delta oscillations as a particularly strong predictor of visual-target detection (Fig. 3). Within the context of the present experiment, the phase of low-delta oscillations was (1) significantly linked to visual-target detection for all participants and (2) had the strongest link to visual-target detection at the population level (relative to phase-detection relationships at other frequencies). Based on Fiebelkorn et al. (2011), which suggested that hit rates oscillate at a frequency of approximately 1 Hz, we designed the present experiment such that interstimulus intervals would be long enough to measure the prestimulus phase of low-delta oscillations (Fig. 1). Baselines in several previous studies, in comparison, were too short to examine the link between low-delta oscillations and visual-target detection (Busch et al., 2009; Mathewson et al., 2009). The effect sizes reported here for

low-delta—as well as the other frequency bands—compare favorably with previous studies linking theta/low alpha phase to visual-target detection (Busch et al., 2009; Mathewson et al., 2009).

For both delta and theta, the truly dramatic effect that these lower frequencies have on perceptual outcomes was revealed through their interactions with higher frequencies, particularly in the beta band. These data demonstrate that phase-detection relationships at higher frequencies can be almost entirely dependent on the phase of delta and theta oscillations (Figs. 4 and 5). That is, a higher frequency's phase-detection relationship was consistently strong at one phase of delta (or theta) and weak at the opposite phase of delta (or theta). In a very different experimental context (i.e., during the presentation of natural movies), Whittingstall and Logothetis (2009) reported a similar coupling between phase in the delta band (2–4 Hz) and the relationship between gamma (30–100 Hz) power and neuronal spiking in monkey visual cortex. Their results demonstrated that gamma power was only tied to increased or decreased spiking during the negative-going phase of delta oscillations (and not during the positive-going phase). In both the present study and Whittingstall and Logothetis (2009), the phase of lower-frequency oscillations seems to act like a switch, controlling whether higher frequency oscillations exert their influence on neurophysiological and perceptual outcomes.

Top-down attention and neurophysiological context

It is well-established that cognitive (or top-down) processes can modulate the phase (Fiebelkorn et al., 2011; Lakatos et al., 2008, 2009) and power of ongoing oscillations (Foxe et al., 1998; Kelly et al., 2006; Sauseng et al., 2005; Snyder and Foxe, 2010; Thut et al., 2006; Worden et al., 2000). Top-down attention has also been associated with increased oscillatory synchronization across a frontoparietal network, particularly increased synchronization within the beta band (Buschman and Miller, 2007; Gross et al., 2004; Hipp et al., 2011; Pesaran et al., 2008). Buschman and Miller (2007), for example, trained non-human primates to detect a visual target amid a set of distractors under either a pop-out or serial search regime. Under both conditions, their results showed increased synchronization between frontal and parietal signals, but during the more endogenously driven serial search, this synchronization was strongest in the high-beta band (22–34 Hz). In the present study, we investigated the link between oscillatory phase and visual-target detection in the context of a sustained-attention task. Our results seem to similarly suggest the involvement of frontal regions, with the phase of beta at the front of the scalp being strongly linked with perceptual outcomes (Fig. 6). Indeed, one of the more prominent peaks in the phase-detection relationships occurred in the high-beta band (21–25 Hz), which is in good agreement with the results of Buschman and Miller (2007).

A question that remains open to interpretation is how synchronized oscillatory activity in the frontoparietal network leads to enhanced processing of sensory stimulation? Several different viewpoints bear on this issue: (1) that perception is discrete rather than continuous (VanRullen and Koch, 2003; VanRullen et al., 2006), (2) that synchronization within high-frequency local oscillations reflects sensory selection (Fries, 2009; Fries et al., 2001, 2002; Gray et al., 1989), and (3) that low-frequency oscillations, which are often associated with long-range synchronization, also have an important role in sensory selection (Fiebelkorn et al., 2011; Gomez-Ramirez et al., 2011; Kayser et al., 2008; Lakatos et al., 2007, 2008; Schroeder and Lakatos, 2009). Combining these viewpoints, we posit that high-frequency ongoing oscillations in the sensory cortices reflect discrete sampling of the environment. This process must occur at a high enough frequency that discrete sampling goes unnoticed by the observer (a concept referred to as "flicker fusion" in vision). When information is available regarding the spatial location or time period when a task-relevant stimulus might occur, the frontoparietal network, which operates at low frequencies, can endogenously depolarize neuronal ensembles in the sensory cortices. Low-frequency depolarization across a patch of cortex resets the phase of local high-frequency oscillations, increasing synchronization. Local high-frequency oscillations thus become embedded in endogenous low-frequency oscillations, and both local and endogenous frequencies contribute to whether the response to a predictable stimulus clears the threshold for detection.

Inter-participant differences

All seven participants demonstrated significant phase-detection relationships across a wide range of frequencies, and there was good agreement in terms of the frequency bands where peaks in these phase-detection relationships occurred (Figs. 3–5). On the other hand, the specific frequencies where peaks occurred and the spatial distribution of the underlying oscillators (on the scalp) were more variable. The extent to which such variability across participants is typical or atypical remains largely unknown because (1) few EEG studies present participant-level data, and (2) the topographies depicted in the present experiment illustrate the strength and location of significant phase-detection relationships, rather than a more common oscillatory measure (such as oscillatory amplitude). Here, we included participant-level data and statistics because we believe that the apparent variability across participants (in the context of the present experiment) largely arises from functionally relevant differences, rather than measurement noise. Such inter-participant variability might arise from multiple origins, including: (1) neuroanatomic differences, such as cortical folding and path lengths, and (2) differences in cognitive strategies or attentional engagement that might influence the brain networks most closely linked to the likelihood of visual-target detection.

Anatomical differences in cortical folding lead to considerable variability in how signals at various frequencies sum at the scalp, or even variability as to whether signals from various neuronal ensembles (or brain regions) are represented on the scalp at all (Di Russo et al., 2002). Different path lengths, on the other hand, might account for slight differences in the specific frequency (e.g., 23 Hz) that was most closely associated with visual-target detection within a more broadly defined frequency band (e.g., beta). Previous studies have similarly demonstrated inter-participant variability in the specific frequencies where synchronization occurs (Dockree et al., 2007; Lykken et al., 1974; Sehatpour et al., 2008). Such variability in center frequencies might arise from variability in brain size, which influences the resonant frequencies within and between cortical regions that emerge from participant-specific neuronal architecture.

A second potential source of inter-participant variability (i.e., differences in cognitive strategies or attentional engagement) might contribute to the spatial distribution of oscillators with significant phase-detection relationships. That is, differences in how each participant engages in the experimental task, might lead to variability in the specific brain regions and oscillatory frequencies that are most strongly linked to the likelihood of visual-target detection. Top-down attention, for example, leads to increased activity within a network that includes superior frontal cortex and parts of the intraparietal cortex; whereas, bottom-up attentional capture activates a right-lateralized network that includes inferior frontal cortex and temporoparietal cortex (Corbetta and Shulman, 2002). In the present experiment, we asked participants to focus their attentional resources for more than 5 s, but we only analyzed trials when the near-threshold visual target was presented at least 2.5 s after the auditory cue (Fig. 1). It is therefore possible that some variability in the spatial distribution of oscillators reflects the extent to which participants were able to consistently sustain attention throughout the duration of a trial.

Future research will need to examine whether slight variations in an experimental task either increase or decrease inter-participant variability in the spectral architecture associated with perceptual and behavioral outcomes. In summary, population-level statistics

revealed systematic phase-detection relationships across many of the same frequency bands that are typically discussed in the literature. The fact that participant-level statistics revealed significant phase-detection relationships (or peaks) at only a subset of these frequency bands (for each participant) is a notable finding that requires further investigation.

Conclusion

Although previous studies in both animals and humans have described cross-frequency coupling between multiple pairs of oscillatory frequencies (Belluscio et al., 2012; Bragin et al., 1995; Canolty and Knight, 2010; Canolty et al., 2006; Cohen et al., 2008; Csicsvari et al., 2003; Handel and Haarmeier, 2009; Jensen and Colgin, 2007; Lakatos et al., 2005; Palva et al., 2005; Schack et al., 2002), the present data provide the first demonstration that such coupling has significant consequences for perceptual outcomes. The data further reveal that the specific higher frequencies and scalp sites predicting visual-target detection vary across the "good" phase of the lower-frequency oscillation (i.e., the phase with the highest likelihood of visual-target detection) and the "bad" phase of the lower-frequency oscillation (i.e., the phase with the lowest likelihood of visual-target detection). In other words, these data reveal that the specific higher frequencies and scalp topographies linked to visual-target detection shift as a function of lower-frequency phase (Fig. 6), hinting at important network dynamics that will require further investigation.

Acknowledgments

This work was supported by a National Institute of Mental Health grant MH-085322 to SM and JJF, and a National Science Foundation grant BCS0642584 to JJF. MRM received additional support from the Swiss National Science Foundation (PBELP3-123067). ACS was supported by a grant from the National Institute of Mental Health (F31 MH-087077). We would like to thank Dr. Scott Makeig and Dr. Peter Lakatos for providing insightful comments on an earlier version of this manuscript. Finally, we would like to thank and remember our dear friend, Dr. Josh Wallman, who served on the doctoral committees of both ICF and ACS. His enthusiasm and passion for scientific discovery continues to inspire, and we are grateful for the time we spent with him and the knowledge he bestowed on us.

References

Arieli, A., Sterkin, A., Grinvald, A., Aertsen, A., 1996. Dynamics of ongoing activity: explanation of the large variability in evoked cortical responses. Science 273, 1868–1871.
Belluscio, M.A., Mizuseki, K., Schmidt, R., Kempter, R., Buzsaki, G., 2012. Cross-frequency phase-phase coupling between theta and gamma oscillations in the hippocampus. J. Neurosci. 32, 423–435.
Benjamini, Y., Hochberg, Y., 1995. Controlling the false discovery rate—a practical and powerful approach to multiple testing. J. R. Stat. Soc.: Ser. B: Methodol. 57, 289–300.
Besle, J., Schevon, C.A., Mehta, A.D., Lakatos, P., Goodman, R.R., McKhann, G.M., Emerson, R.G., Schroeder, C.E., 2011. Tuning of the human neocortex to the temporal dynamics of attended events. J. Neurosci. 31, 3176–3185.
Boly, M., Balteau, E., Schnakers, C., Degueldre, C., Moonen, G., Luxen, A., Phillips, C., Peigneux, P., Maquet, P., Laureys, S., 2007. Baseline brain activity fluctuations predict somatosensory perception in humans. Proc. Natl. Acad. Sci. U. S. A. 104, 12187–12192.
Bragin, A., Jando, G., Nadasdy, Z., Hetke, J., Wise, K., Buzsaki, G., 1995. Gamma (40–100 Hz) oscillation in the hippocampus of the behaving rat. J. Neurosci. 15, 47–60.
Busch, N.A., VanRullen, R., 2010. Spontaneous EEG oscillations reveal periodic sampling of visual attention. Proc. Natl. Acad. Sci. U.S.A. 107, 16048–16053.
Busch, N.A., Dubois, J., VanRullen, R., 2009. The phase of ongoing EEG oscillations predicts visual perception. J. Neurosci. 29, 7869–7876.
Buschman, T.J., Miller, E.K., 2007. Top-down versus bottom-up control of attention in the prefrontal and posterior parietal cortices. Science 315, 1860–1862.
Buzsaki, G., Chrobak, J.J., 1995. Temporal structure in spatially organized neuronal ensembles: a role for interneuronal networks. Curr. Opin. Neurobiol. 5, 504–510.
Canolty, R.T., Knight, R.T., 2010. The functional role of cross-frequency coupling. Trends Cogn. Sci. 14, 506–515.
Canolty, R.T., Edwards, E., Dalal, S.S., Soltani, M., Nagarajan, S.S., Kirsch, H.E., Berger, M.S., Barbaro, N.M., Knight, R.T., 2006. High gamma power is phase-locked to theta oscillations in human neocortex. Science 313, 1626–1628.
Cohen, M.X., Ridderinkhof, K.R., Haupt, S., Elger, C.E., Fell, J., 2008. Medial frontal cortex and response conflict: evidence from human intracranial EEG and medial frontal cortex lesion. Brain Res. 1238, 127–142.
Corbetta, M., Shulman, G.L., 2002. Control of goal-directed and stimulus-driven attention in the brain. Nat. Rev. Neurosci. 3, 201–215.
Csicsvari, J., Jamieson, B., Wise, K.D., Buzsaki, G., 2003. Mechanisms of gamma oscillations in the hippocampus of the behaving rat. Neuron 37, 311–322.
Di Russo, F., Martinez, A., Sereno, M.I., Pitzalis, S., Hillyard, S.A., 2002. Cortical sources of the early components of the visual evoked potential. Hum. Brain Mapp. 15, 95–111.
Dockree, P.M., Kelly, S.P., Foxe, J.J., Reilly, R.B., Robertson, I.H., 2007. Optimal sustained attention is linked to the spectral content of background EEG activity: greater ongoing tonic alpha (approximately 10 Hz) power supports successful phasic goal activation. Eur. J. Neurosci. 25, 900–907.
Dugue, L., Marque, P., VanRullen, R., 2011. The phase of ongoing oscillations mediates the causal relation between brain excitation and visual perception. J. Neurosci. 31, 11889–11893.
Fiebelkorn, I.C., Foxe, J.J., Butler, J.S., Mercier, M.R., Snyder, A.C., Molholm, S., 2011. Ready, set, reset: stimulus-locked periodicity in behavioral performance demonstrates the consequences of cross-sensory phase reset. J. Neurosci. 31, 9971–9981.
Foxe, J.J., Simpson, G.V., Ahlfors, S.P., 1998. Parieto-occipital similar to 10 Hz activity reflects anticipatory state of visual attention mechanisms. Neuroreport 9, 3929–3933.
Fries, P., 2009. Neuronal gamma-band synchronization as a fundamental process in cortical computation. Annu. Rev. Neurosci. 32, 209–224.
Fries, P., Reynolds, J.H., Rorie, A.E., Desimone, R., 2001. Modulation of oscillatory neuronal synchronization by selective visual attention. Science 291, 1560–1563.
Fries, P., Schroder, J.H., Roelfsema, P.R., Singer, W., Engel, A.K., 2002. Oscillatory neuronal synchronization in primary visual cortex as a correlate of stimulus selection. J. Neurosci. 22, 3739–3754.
Genovese, C.R., Lazar, N.A., Nichols, T., 2002. Thresholding of statistical maps in functional neuroimaging using the false discovery rate. NeuroImage 15, 870–878.
Gomez-Ramirez, M., Kelly, S.P., Molholm, S., Sehatpour, P., Schwartz, T.H., Foxe, J.J., 2011. Oscillatory sensory selection mechanisms during intersensory attention to rhythmic auditory and visual inputs: a human electrocorticographic investigation. J. Neurosci. 31, 18556–18567.
Gray, C.M., Konig, P., Engel, A.K., Singer, W., 1989. Oscillatory responses in cat visual cortex exhibit inter-columnar synchronization which reflects global stimulus properties. Nature 338, 334–337.
Groppe, D.M., Urbach, T.P., Kutas, M., 2011. Mass univariate analysis of event-related brain potentials/fields I: a critical tutorial review. Psychophysiology 48, 1711–1725.
Gross, J., Schmitz, F., Schnitzler, I., Kessler, K., Shapiro, K., Hommel, B., Schnitzler, A., 2004. Modulation of long-range neural synchrony reflects temporal limitations of visual attention in humans. Proc. Natl. Acad. Sci. U.S.A. 101, 13050–13055.
Haig, A.R., Gordon, E., 1998. EEG alpha phase at stimulus onset significantly affects the amplitude of the P3 ERP component. Int. J. Neurosci. 93 (101-+).
Handel, B., Haarmeier, T., 2009. Cross-frequency coupling of brain oscillations indicates the success in visual motion discrimination. NeuroImage 45, 1040–1046.
Hipp, J.F., Engel, A.K., Siegel, M., 2011. Oscillatory synchronization in large-scale cortical networks predicts perception. Neuron 69, 387–396.
Jansen, B.H., Brandt, M.E., 1991. The effect of the phase of prestimulus alpha activity on the averaged visual evoked response. Electroencephalogr. Clin. Neurophysiol. 80, 241–250.
Jensen, O., Colgin, L.L., 2007. Cross-frequency coupling between neuronal oscillations. Trends Cogn. Sci. 11, 267–269.
Kastner, S., Pinsk, M.A., De Weerd, P., Desimone, R., Ungerleider, L.G., 1999. Increased activity in human visual cortex during directed attention in the absence of visual stimulation. Neuron 22, 751–761.
Kayser, C., Petkov, C.I., Logothetis, N.K., 2008. Visual modulation of neurons in auditory cortex. Cereb. Cortex 18, 1560–1574.
Kelly, S.P., Lalor, E.C., Reilly, R.B., Foxe, J.J., 2006. Increases in alpha oscillatory power reflect an active retinotopic mechanism for distracter suppression during sustained visuospatial attention. J. Neurophysiol. 95, 3844–3851.
Kruglikov, S.Y., Schiff, S.J., 2003. Interplay of electroencephalogram phase and auditory-evoked neural activity. J. Neurosci. 23, 10122–10127.
Lakatos, P., Shah, A.S., Knuth, K.H., Ulbert, I., Karmos, G., Schroeder, C.E., 2005. An oscillatory hierarchy controlling neuronal excitability and stimulus processing in the auditory cortex. J. Neurophysiol. 94, 1904–1911.
Lakatos, P., Chen, C.M., O'Connell, M.N., Mills, A., Schroeder, C.E., 2007. Neuronal oscillations and multisensory interaction in primary auditory cortex. Neuron 53, 279–292.
Lakatos, P., Karmos, G., Mehta, A.D., Ulbert, I., Schroeder, C.E., 2008. Entrainment of neuronal oscillations as a mechanism of attentional selection. Science 320, 110–113.
Lakatos, P., O'Connell, M.N., Barczak, A., Mills, A., Javitt, D.C., Schroeder, C.E., 2009. The leading sense: supramodal control of neurophysiological context by attention. Neuron 64, 419–430.
Lange, J., Halacz, J., van Dijk, H., Kahlbrock, N., Schnitzler, A., 2011. Fluctuations of prestimulus oscillatory power predict subjective perception of tactile simultaneity. Cereb. Cortex 22, 2564–2574.
Lykken, D.T., Tellegen, A., Thorkelson, K., 1974. Genetic determination of EEG frequency spectra. Biol. Psychol. 1, 245–259.
Makeig, S., Westerfield, M., Jung, T.P., Enghoff, S., Townsend, J., Courchesne, E., Sejnowski, T.J., 2002. Dynamic brain sources of visual evoked responses. Science 295, 690–694.
Mathewson, K.E., Gratton, G., Fabiani, M., Beck, D.M., Ro, T., 2009. To see or not to see: prestimulus alpha phase predicts visual awareness. J. Neurosci. 29, 2725–2732.
McMains, S.A., Fehd, H.M., Emmanouil, T.A., Kastner, S., 2007. Mechanisms of feature- and space-based attention: response modulation and baseline increases. J. Neurophysiol. 98, 2110–2121.

Monto, S., Palva, S., Voipio, J., Palva, J.M., 2008. Very slow EEG fluctuations predict the dynamics of stimulus detection and oscillation amplitudes in humans. J. Neurosci. 28, 8268–8272.
O'Connell, R.G., Dockree, P.M., Robertson, I.H., Bellgrove, M.A., Foxe, J.J., Kelly, S.P., 2009. Uncovering the neural signature of lapsing attention: electrophysiological signals predict errors up to 20 s before they occur. J. Neurosci. 29, 8604–8611.
Palva, J.M., Palva, S., Kaila, K., 2005. Phase synchrony among neuronal oscillations in the human cortex. J. Neurosci. 25, 3962–3972.
Pesaran, B., Nelson, M.J., Andersen, R.A., 2008. Free choice activates a decision circuit between frontal and parietal cortex. Nature 453, 406–409.
Romei, V., Brodbeck, V., Michel, C., Amedi, A., Pascual-Leone, A., Thut, G., 2008. Spontaneous fluctuations in posterior alpha-band EEG activity reflect variability in excitability of human visual areas. Cereb. Cortex 18, 2010–2018.
Sadaghiani, S., Scheeringa, R., Lehongre, K., Morillon, B., Giraud, A.L., Kleinschmidt, A., 2010. Intrinsic connectivity networks, alpha oscillations, and tonic alertness: a simultaneous electroencephalography/functional magnetic resonance imaging study. J. Neurosci. 30, 10243–10250.
Sauseng, P., Klimesch, W., Stadler, W., Schabus, M., Doppelmayr, M., Hanslmayr, S., Gruber, W.R., Birbaumer, N., 2005. A shift of visual spatial attention is selectively associated with human EEG alpha activity. Eur. J. Neurosci. 22, 2917–2926.
Schack, B., Vath, N., Petsche, H., Geissler, H.G., Moller, E., 2002. Phase-coupling of theta-gamma EEG rhythms during short-term memory processing. Int. J. Psychophysiol. 44, 143–163.
Scheeringa, R., Mazaheri, A., Bojak, I., Norris, D.G., Kleinschmidt, A., 2011. Modulation of visually evoked cortical FMRI responses by phase of ongoing occipital alpha oscillations. J. Neurosci. 31, 3813–3820.
Schroeder, C.E., Lakatos, P., 2009. Low-frequency neuronal oscillations as instruments of sensory selection. Trends Neurosci. 32, 9–18.
Sehatpour, P., Molholm, S., Schwartz, T.H., Mahoney, J.R., Mehta, A.D., Javitt, D.C., Stanton, P.K., Foxe, J.J., 2008. A human intracranial study of long-range oscillatory coherence across a frontal–occipital–hippocampal brain network during visual object processing. Proc. Natl. Acad. Sci. U.S.A. 105, 4399–4404.
Snyder, A.C., Foxe, J.J., 2010. Anticipatory attentional suppression of visual features indexed by oscillatory alpha-band power increases: a high-density electrical mapping study. J. Neurosci. 30, 4024–4032.
Thut, G., Nietzel, A., Brandt, S.A., Pascual-Leone, A., 2006. Alpha-band electroencephalographic activity over occipital cortex indexes visuospatial attention bias and predicts visual target detection. J. Neurosci. 26, 9494–9502.
VanRullen, R., Koch, C., 2003. Is perception discrete or continuous? Trends Cogn. Sci. 7, 207–213.
VanRullen, R., Reddy, L., Koch, C., 2006. The continuous wagon wheel illusion is associated with changes in electroencephalogram power at approximately 13 Hz. J. Neurosci. 26, 502–507.
Varela, F.J., Toro, A., John, E.R., Schwartz, E.L., 1981. Perceptual framing and cortical alpha rhythm. Neuropsychologia 19, 675–686.
von Stein, A., Sarnthein, J., 2000. Different frequencies for different scales of cortical integration: from local gamma to long range alpha/theta synchronization. Int. J. Psychophysiol. 38, 301–313.
Whittingstall, K., Logothetis, N.K., 2009. Frequency-band coupling in surface EEG reflects spiking activity in monkey visual cortex. Neuron 64, 281–289.
Worden, M.S., Foxe, J.J., Wang, N., Simpson, G.V., 2000. Anticipatory biasing of visuospatial attention indexed by retinotopically specific alpha-band electroencephalography increases over occipital cortex. J. Neurosci. 20, RC63.